Glycobiology vol. 17 no. 8 pp. 828–837, 2007
doi:10.1093/glycob/cwm048
Advance Access publication on May 4, 2007

Metabolic homeostasis and tissue renewal are dependent on β1,6GlcNAc-branched *N*-glycans

Pam Cheung[2,3], Judy Pawling[2], Emily A Partridge[2,4], Balram Sukhu[2], Marc Grynpas[2,4], and James W Dennis[1,3,4]

[2]Samuel Lunenfeld Research Institute, Mount Sinai Hospital, 600 University Avenue R988, Toronto, ON, Canada M5G 1X5; [3]Department of Molecular and Medical Genetics and [4]Department of Laboratory Medicine and Pathology, University of Toronto, Canada

Received on January 25, 2007; revised on March 22, 2007; accepted on April 19, 2007

Golgi β1,6-*N*-acetylglucosaminyltransferase V (Mgat5) produces β1,6GlcNAc-branched *N*-glycans on glycoproteins, which increases their affinity for galectins and opposes loss from the cell surface to constitutive endocytosis. Oncogenic transformation increases Mgat5 expression, increases β1,6GlcNAc-branched *N*-glycans on epidermal growth factor and transforming growth factor-β receptors, and enhances sensitivities to ligands, cell motility, and tumor metastasis. Here, we demonstrate that Mgat5$^{-/-}$ mouse embryonic fibroblasts (MEFs) display reduced sensitivity to anabolic cytokines and reduced glucose uptake and proliferation. Mgat5$^{-/-}$ mice are also hypoglycemic, resistant to weight gain on a calorie-enriched diet, hypersensitive to fasting, and display increased oxidative respiration and reduced fecundity. Serum-dependent activation of the extracellular response kinase (growth) and Smad2/3 (arrest) pathways in Mgat5$^{-/-}$ MEFs and bone marrow cells reveals an imbalance favoring arrest. Mgat5$^{-/-}$ mice have fewer muscle satellite cells, less osteogenic activity in bone marrow, and accelerated loss of muscle and bone mass with aging. Our results suggest that β1,6GlcNAc-branched *N*-glycans promote sensitivity to anabolic cytokines, and increase fat stores, tissue renewal, and longevity.

Key words: aging/cytokine signaling/metabolism/Mgat5/*N*-glycans/stem cells

Introduction

Glucose is a ligand for a family of signaling receptors in *Saccharomyces cerevisiae* that couples metabolism with cell replication, filamentous invasive growth, and balanced oxidative and fermentative metabolism (Ozcan et al. 1998; Rolland et al. 2000). Although downstream intracellular nutrient-sensing pathways (i.e. Akt/Sch9 and Ras-cAMP) are largely conserved in eukaryotes (Sobko 2006), growth signaling in metazoan cells is stimulated by extracellular cytokine and receptor tyrosine kinases (RTKs), as required to specify their complex body plans (Di Paolo and De Camilli 2006). However equally important are signaling pathways that limit growth and are sensitive to extracellular morphogens such as the transforming growth factor-β (TGF-β)/bone morphogenic protein (BMP) family (Wakefield and Roberts 2002). TGF-β receptor (TβR)/Smad and RTK/PI3K/extracellular response kinase (Erk) pathways interact at multiple levels and, ultimately, the former promotes cell cycle arrest by decreasing c-Myc and increasing $p21^{Cip1}$ and $p15^{INK4a}$ expressions (Siegel and Massague 2003; Seoane et al. 2004). For example, self-renewal and pluripotency of cultured human embryonic stem cells is optimally preserved by precise proportions of basic fibroblast growth factor (bFGF) and Noggin, a BMP/TGF-β antagonist (Xu et al. 2005). BMP4 alone can shift the equilibrium toward differentiation, as has been shown for tumor-initiating stem cells, thereby inhibiting human glioblastoma growth in mice (Piccirillo et al. 2006). The availability of receptors for insulin and epidermal growth factor (EGF) and platelet derived growth factor (PDGF) cytokines decline with age in primary cells, which may also limit the incidence of cancers while contributing to the loss of renewal with age (Yeo and Park 2002). As such, growth factors promote tissue renewal and metabolism with aging, and their action is balanced by growth-suppressing pathways that limit cancer risk (Campisi 2005; Conboy et al. 2005). Imbalances, such as the loss of the DNA damage checkpoint protein p53, relieve a brake on proliferation and glycolytic metabolism, and increase the risk of cancer but also increase longevity for individuals remaining cancer-free (Tyner et al. 2002; van Heemst et al. 2005; Matoba et al. 2006).

We have recently shown that adaptive changes in *N*-glycan processing in mammalian cells downstream of metabolic flux to sugar nucleotides regulate surface receptors and cellular sensitivities to cytokines (Lau et al. 2007). Glucose, acetyl-CoA, and glutamine are substrates of the hexosamine pathway to UDP-GlcNAc, a key substrate in the biosynthesis of complex *N*-glycans found on cell surface receptors and transporters (Sasai et al. 2002; Grigorian et al. 2007). *N*-acetylglucosaminyltransferases I, II, III, IV, and V (GlcNAc-Ts) (encoded by β1,6-*N*-acetylglucosaminyl transferases Mgat1, Mgat2, Mgat3, Mgat4a/b, and Mgat5) act sequentially in the medial Golgi to initiate the *N*-acetyllactosamine branches on complex *N*-glycans. End products of the pathway, the β1,6GlcNAc-branched tetra-antennary *N*-glycans, are higher

[1]To whom correspondence should be addressed; Tel: +1-416-586-8233; Fax: +1-416-586-8588; e-mail: dennis@mshri.on.ca.

affinity ligands for galectins-3 and -9 compared with the less branched structures (Hirabayashi et al. 2002; Lau et al. 2007). Galectins bind and cross-link complex *N*-glycans on receptors at the cells surface (Demetriou et al. 2001; Brewer et al. 2002) which enhances their surface residency (Partridge et al. 2004). In this regard, Mgat5$^{-/-}$ tumor cells display fewer surface EGF and TGF-β receptors, proportionately more in the endosomes, and are less responsive to multiple cytokines (Partridge et al. 2004). Oncogenic transformation increases Mgat5 gene expression (Kang et al. 1996; Buckhaults et al. 1997), and β1,6GlcNAc-branching of *N*-glycans is associated with a poor prognosis in human patients (Fernandes et al. 1991; Seelentag et al. 1998).

We have recently shown that metabolic flux to UDP-GlcNAc and *N*-glycan processing cooperates with *N*-glycan number to regulate cellular sensitivities to cytokines (Lau et al. 2007). The number of *N*-glycans or multiplicity (*n*) is an encoded feature of the protein that differs markedly between different surface glycoproteins. The numbers of potential glycoforms increase exponentially with multiplicity, and these larger molecular distributions have higher median affinities for the galectin lattice. Therefore, high multiplicity can enhance avidity for the lattice even when GlcNAc branching is low, whereas glycoproteins with low multiplicity require more GlcNAc branching for stable association with the lattice. Metabolite flux through the hexosamine pathway to UDP-GlcNAc and medial GlcNAc-Ts increases the tri- and tetra-antennary *N*-glycan content on glycoproteins. Thus, growth factor receptors with high *n* [e.g. EGFR, PDGFR, FGFR, and insulin-like growth factor receptor IGFR] increase at the cell surface first in response to increasing UDP-GlcNAc, followed by low-*n* glycoproteins (e.g. TβR) (Lau et al. 2007). Receptor kinases that stimulate cell proliferation and promote oncogenesis have increased numbers and densities of Asn-X-Ser/Thr (X ≠ Pro) motifs, compared with receptor kinases required for tissue morphogenesis and growth arrest. Computational simulation of *N*-glycan processing and galectin lattice dynamics and experimental data from cell culture models indicate that metabolic flux to *N*-glycan processing regulates the proportions of glycoproteins at the surface and thus cellular responses to multiple cytokines (Lau et al. 2007). We report here that primary Mgat5$^{-/-}$ cells display a signaling imbalance (RTK/PI3K/Erk and TGF-β/Smad) that favors growth arrest. Mgat5-deficient mice are resistant to weight gain on a calorie-enriched diet, and display increased oxidative respiration, reduced osteogenic activity and muscle satellite cells, and an early aging phenotype. Our results suggest that conditional expression of β1,6GlcNAc-branched *N*-glycans in postnatal tissues promotes anabolic metabolism and tissue renewal by adapting cellular sensitivities to growth and arrest cues.

Results

Mgat5-modified N-*glycans promote glucose uptake and sensitivity to growth factors*

If the loss of cytokine sensitivity observed in polyomavirus middle T Mgat5$^{-/-}$ tumor cells (Partridge et al. 2004) is also present in primary cells from Mgat5$^{-/-}$ mice, we might anticipate a chronic deficiency in growth signaling and suppression of glucose metabolism. Indeed, Erk-p nuclear translocation in response to EGF, PDGF, FGF, and IGF cytokines was suppressed in Mgat5$^{-/-}$ compared with Mgat5$^{+/+}$ mouse embryonic fibroblasts (MEFs) (Figure 1A). Basal levels of activated Akt and Erk were reduced in Mgat5$^{-/-}$ MEFs, and doubling time increased under normal culture conditions (Figure 1B, data not shown). Glucose uptake rates and reactive oxygen species (ROS) levels were similar in Mgat5$^{-/-}$ and Mgat5$^{+/+}$ MEFs growing in high-glucose and high-fetal calf serum (FCS) conditions. However, either low-glucose or serum-free medium (SFM) conditions revealed Mgat5$^{-/-}$ MEFs as deficient in both, suggesting that Mgat5-modified *N*-glycans promote glucose metabolism (Figure 1C and D). Glucose transport is increased by low-glucose conditions and by serum in an additive manner (Figure 1C). Mgat5$^{-/-}$ MEFs proliferate more slowly and are less responsive to increasing serum concentrations in the growth medium, consistent with their deficiency in acute responses to growth factors (Figure 1E). Thus, Mgat5-modified *N*-glycans sensitize primary non-transformed cells to extrinsic growth cues, increase basal PI3K/Erk activation, and promote glucose uptake and metabolism. Indeed, cell surface β1,6 GlcNAc-branched

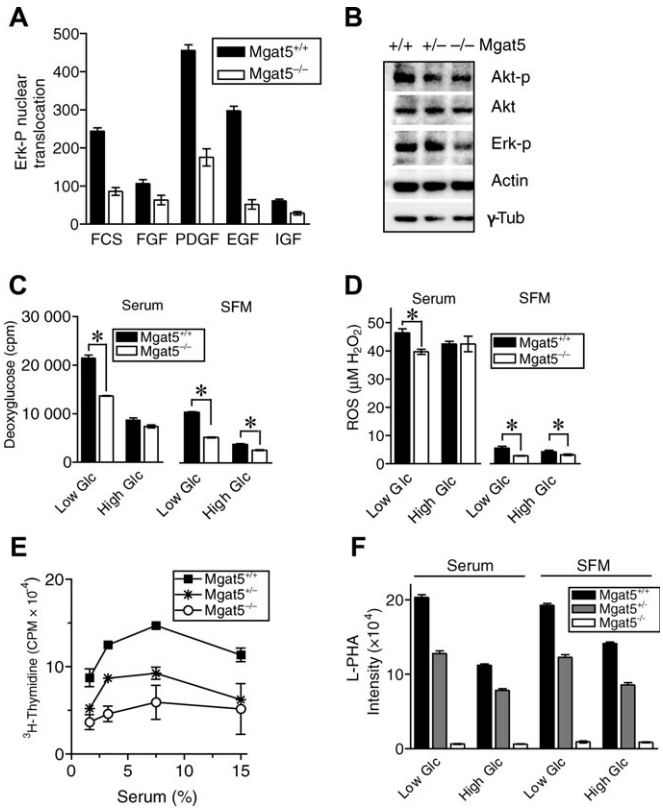

Fig. 1. Cytokine responsiveness, proliferation, glucose uptake, and ROS are dependent on Mgat5 in MEFs. (**A**) Erk-p nuclear translocation in serum-starved MEFs following stimulation with serum (10%) or cytokines (100 ng/mL) and measured by ArrayScan Cellomics, Pittsburgh. (**B**) Western blot of lysates from Mgat5$^{+/+}$, Mgat5$^{+/-}$, and Mgat5$^{-/-}$ MEFs cultured in DMEM and 10% FCS. (**C**) [^{3}H]2-Deoxyglucose uptake and (**D**) ROS levels in MEFs grown for 24 h in the indicated conditions of low glucose (0.5 mM), high glucose (25 mM), SFM, and 10% serum (mean ± SD, $n = 6$). *$P < 0.05$ pairwise comparisons. (**E**) MEF proliferation measured by pulse labeling with [^{3}H]thymidine for the final 24 h of a 2-day culture period. (**F**) MEFs were cultured under high-and low-glucose conditions for 24 h and then in the presence and absence of serum for an additional 24 h and stained with FITC-labeled plant lectin L-PHA, and the mean ± SD for six replicates was measured by ArrayScan.

N-glycans increase under restricted glucose concentrations compared with excess glucose concentrations (Figure 1F). This indicates that *N*-glycan branching is sensitive to upregulation by glucose deprivation, which may be the result of altered hexosamine flux, increased expression of Golgi enzymes, or altered trafficking of glycoproteins.

Resistance to obesity in Mgat5-deficient mice

To determine whether Mgat5 is a determinant of metabolic homeostasis, mutant and wild-type mice on a C57BL/6 background were provided with either regular or high-fat and carbohydrate-enriched diet. Mgat5$^{-/-}$ mice are born in the expected Mendelian ratio from heterozygous matings, normal in proportions and weight, and appear healthy as young adults. Time to weaning was similar for all genotypes on either diet; however, 16 weeks after weaning, male and female Mgat5$^{+/+}$ mice on the enriched diet were approximately 20–30% heavier than Mgat5$^{-/-}$ mice (Figure 2A and B). To assess rates of weight gain in adults, mice raised on the regular diet were transferred to the enriched diet for 6 weeks. Mgat5$^{+/+}$, Mgat5$^{+/-}$, and Mgat5$^{-/-}$ male mice on the enriched diet gained weight at rates of 2.1, 1.7, and 0.3% per week, respectively (Figure 2C). Female mice showed similar weight gains for the respective genotypes (Figure 2D). Mgat5$^{+/-}$ and Mgat5$^{+/+}$ mice born to Mgat5$^{+/-}$ mothers on the enriched food and continued on the same diet were approximately 35% heavier than their Mgat5$^{-/-}$ littermates by approximately 8 months of age (Figure 2E and F). These Mgat5$^{+/-}$ and Mgat5$^{+/+}$ mice lost approximately 10% of their body weight in 6 weeks when switched from the enriched diet to the regular diet, but regained 15–20% in only 5 weeks upon returning to the enriched diet. The body weights of Mgat5$^{-/-}$ mice were remarkably stable despite changes in their diet. Mgat5$^{+/+}$ and Mgat5$^{+/-}$ mice on the enriched diet showed large abdominal fat deposits, whereas Mgat5$^{-/-}$ mice were lean with small fat pads in the groin (not shown). However, Mgat5$^{-/-}$ and Mgat5$^{+/+}$ mice maintained similar daily energy intakes on either the regular or enriched diets (Figure 3A).

Mgat5$^{+/+}$ and Mgat5$^{+/-}$ male mice maintained on the enriched diet displayed elevated nonfasting blood glucose, whereas the Mgat5 deficiency blunted the effect of this diet. Nonfasting blood glucose was reduced in male and female Mgat5$^{-/-}$ mice on both diets (Figure 3B). The enriched diet produced a 36 and 66% increase in blood glucose in male Mgat5$^{-/-}$ and Mgat5$^{+/+}$ mice, respectively. Glucose tolerance tests showed similar kinetics for glucose clearance in Mgat5$^{+/+}$, Mgat5$^{+/-}$, and Mgat5$^{-/-}$ mice, with mutant mice returning to

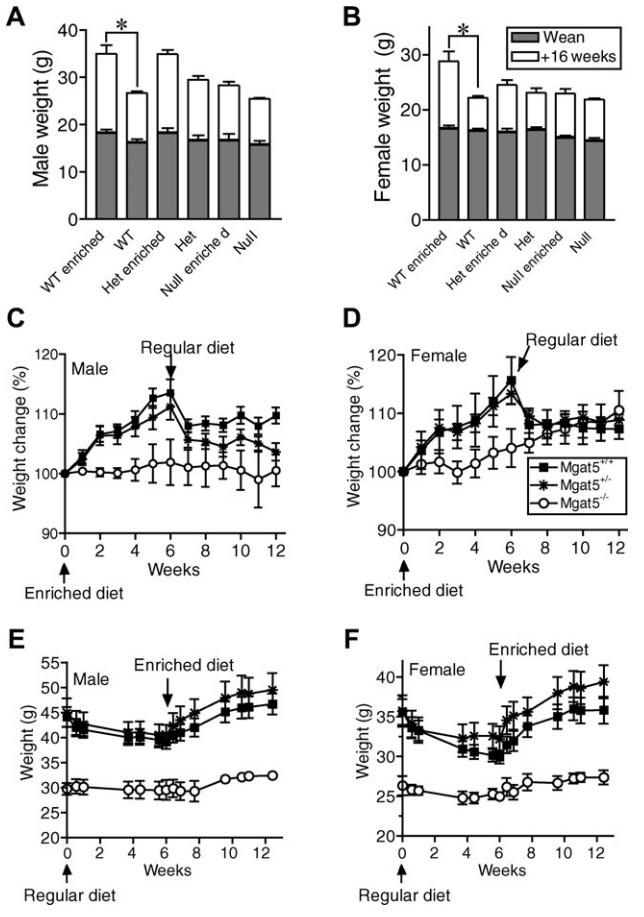

Fig. 2. Mgat5-deficient mice are resistant to obesity on an enriched diet. [(**A**) and (**B**)] Body weights of C57BL/6 male and female mice at weaning (4 weeks, gray) and at 20 weeks of age (white), fed with either regular chow or an enriched diet ad libitum. [(**C**) and (**D**)] Body weights of male and female mice maintained on the enriched diets, beginning in utero, then changed at 8 months of age to the regular diet for 6 weeks, and back to the enriched diet for a further 6 weeks. [(**E**) and (**F**)] Body weight of male and female mice maintained on the regular diet and switched to the enriched diet at around 1 year of age. Mice were on the enriched diet for 6 weeks and then returned to the regular diet.

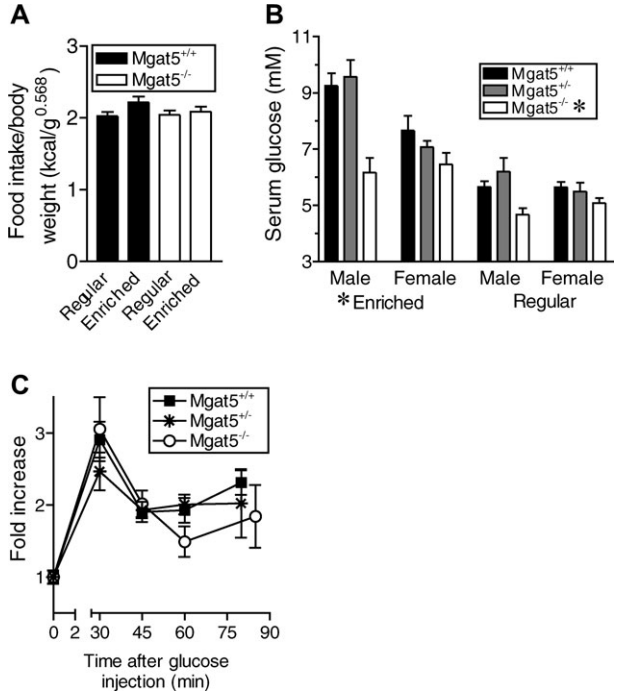

Fig. 3. Mgat5-deficient mice are hypoglycemic. (**A**) Daily calorie intake by C57BL/6 Mgat5$^{+/+}$ and Mgat5$^{-/-}$ mice on the regular and enriched diets (mean ± SE, six mice/group, seven daily measurements). (**B**) Blood glucose levels in male and female mice fed the enriched and regular diets ad libitum (mean ± SE, 4–16 measurements/group). *$P < 0.05$ in a two-way ANOVA comparing diet and genotype separately. (**C**) Glucose tolerance test after 16 h of fasting. Change in serum glucose over time following an IP injection of glucose at 1.5 mg/g body weight.

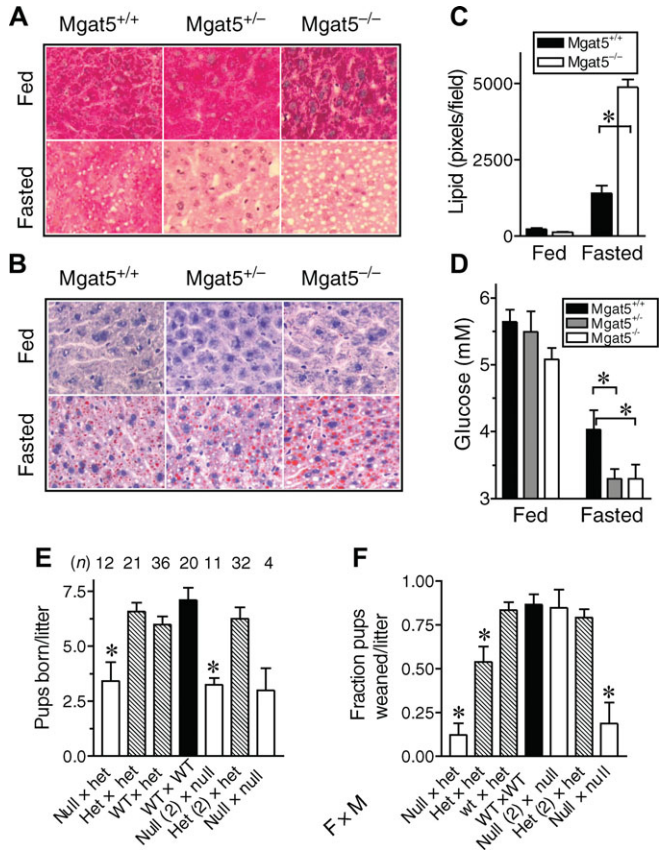

Fig. 4. Mgat5-deficient mice are hypersensitive to fasting. C57BL/6 mice fed on the regular diet or fasted for 20 h were prepared for (**A**) liver glycogen staining with periodic acid–Schiff (PAS) (pink), (**B**) liver lipid staining with Oil Red O, and **(C)** quantification by densitometry (mean ± SE, $n = 5$ mice/group). (**D**) Blood glucose levels in fed and fasted female mice; $^*P < 0.05$. (**E**) Live pups per litter born to C57BL/6 female mice (mean ± SE). FxM indicates female and male genotypes, and "(2)" indicates two females housed with one male. (**F**) Survival of pups to weaning (14–18 g at approximately 4 weeks). $^*P < 0.05$ by pairwise comparison.

lower levels than Mgat5$^{+/+}$ mice (Figure 3C). Liver glycogen stores were similar for all genotypes, but after an 18-h fast, Mgat5$^{-/-}$ mice experienced a greater depletion and mobilization of fat stores to the liver (Figure 4A–C). Fasting blood glucose levels fell to lower levels in Mgat5$^{-/-}$ and Mgat5$^{+/-}$ mice than Mgat5$^{+/+}$ mice, suggesting a metabolic abnormality in liver that is enhanced by fasting (Figure 4D).

Mgat5-modified N*-glycans promote fecundity in a nutrient-dependent manner*

Fecundity is sensitive to both dietary and genetic determinants of nutrient availability and therefore might be lower in Mgat5$^{-/-}$ mice. We observe that Mgat5$^{-/-}$ females on the C57BL/6 background produced fewer pups per litter than Mgat5$^{+/+}$ and Mgat5$^{+/-}$ littermates on the regular diet (Figure 4E). Additionally, only 10% of the newborn pups survived to weaning with Mgat5$^{-/-}$ mothers regardless of their genotypes, compared with 80% of pups with Mgat5-expressing mothers (Figure 4F). Mgat5$^{-/-}$ females housed either alone or with a male displayed less time gathering pups and nurturing (Granovsky et al. 2000). It is possible that the Mgat5 deficiency alters certain sensory functions affecting nurturing, as has been suggested for deficiencies in FosB (Brown et al. 1996) and cAMP response element-binding protein (Jin et al. 2005). Interestingly, when two Mgat5$^{-/-}$ mothers are housed together, the number of pups born per litter is not altered, but rearing efficiency is restored to approximately 80%, suggesting that sharing of material and parenting resources improves Mgat5$^{-/-}$ animals' performance (Figure 4F). Selection pressures to maximize productivity per litter lead to strained parental resources and thus create parent–offspring conflicts (Parker et al. 2002; Hager and Johnstone 2003). Mgat5$^{-/-}$ maternal resources appear to be sufficient for smaller litter sizes as indicated by time to weaning, but this may be at the cost of postnatal culling of pups. Mgat5$^{-/-}$ mothers lost all pups in approximately 25% of litters, which may also arise from a programmed response of reduced commitment to small litters (Kilner et al. 2004).

Respiratory quotient

Weight gain requires that more calories be allotted to anabolic metabolism and storage than utilized in basic maintenance, physical activity, and adaptive thermogenesis. On the regular diet, the respiratory quotient (RQ) (VCO_2/VO_2) was reduced in Mgat5$^{-/-}$ mice during the light cycle ($P < 0.001$), but was not significantly lower in the dark cycle (Figure 5A), suggesting that fatty acid oxidation is increased in Mgat5$^{-/-}$ mice, particularly during the sleep cycle. Locomotion and total movement of Mgat5$^{+/+}$ and Mgat5$^{-/-}$ mice throughout the day were similar under controlled nonstressful conditions (Figure 5B). The anorexigenic hormone leptin was 1.81 ± 0.26 ($n = 19$) and 3.25 ± 0.77 ng/mL ($n = 14$) ($P < 0.057$) in mutant and wild-type mice on the regular diet, respectively. Serum insulin was similar at 0.89 ± 0.12 versus 0.91 ± 0.13 ng/mL, but glucagon levels were 41.2 ± 10.7 and $106.7 + 5.0$ pM in Mgat5$^{+/+}$ and Mgat5$^{-/-}$ mice, respectively. Basal and poststress serum corticosterone levels were also not different in Mgat5$^{-/-}$ and Mgat5$^{+/+}$ mice (data not shown). Stearoyl-CoA desaturase mutant mice display a lean phenotype similar to that of Mgat5$^{-/-}$ mice with reduced leptin levels and increased fatty acid oxidation (Dobrzyn et al. 2004). Calorie-restricted animals also display reduced leptin and blood glucose levels, and increased plasma fatty acids and resting oxidative

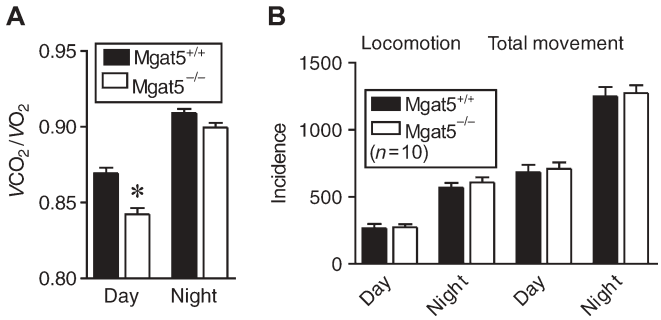

Fig. 5. RQ and activity. (**A**) RQ = VCO_2/VO_2 calculated from oxygen consumption (VO_2) and carbon dioxide production (VCO_2) measured at 15-min intervals and averaged for light and dark cycles over 24 h for 10 mice of each genotype on the regular diet and expressed as RQ ($^*P < 0.001$). (**B**) Locomotion and total movement were measured continuously during the 24 h. Locomotion is a measure of lateral movement, whereas total movement includes body movements such as grooming as well as lateral movement.

metabolism as measured by RQ. Taken together, metabolic homeostasis in Mgat5-deficient mice is characterized by reduced serum glucose and increased catabolic metabolism, suggesting that Mgat5-modified *N*-glycans provide positive feedback to glucose metabolism and fat storage.

Mgat5 promotes renewal in muscle and bone

Mgat5-modified *N*-glycans sensitize MEFs to growth factors and enhance basal glucose uptake in an additive or synergistic manner. If reduced cellular glucose uptake is a characteristic of homeostasis in Mgat5$^{-/-}$ mice, skeletal muscle may display features of chronic starvation, notably increased fast-twitch myofibers, a glycolytic cell type with fewer mitochondria than slow-twitch myofibers (Ryder et al. 2003). Indeed, muscle from 3-month-old Mgat5$^{-/-}$ mice on the regular diet display twice as many fast-twitch myofibers compared with Mgat5$^{+/+}$ muscle (Figure 6A and B). Soft tissue (i.e. largely muscle) and adipose tissue increase in Mgat5$^{+/+}$ mice between 3 and approximately 16 months of age, but remain unchanged in Mgat5$^{-/-}$ littermates, suggesting an accelerated loss of tissue repair and growth with aging (Figure 6C). Serum levels of Na^+, K^+, Ca^{++}, Cl^-, lactate, glutamine, and urea

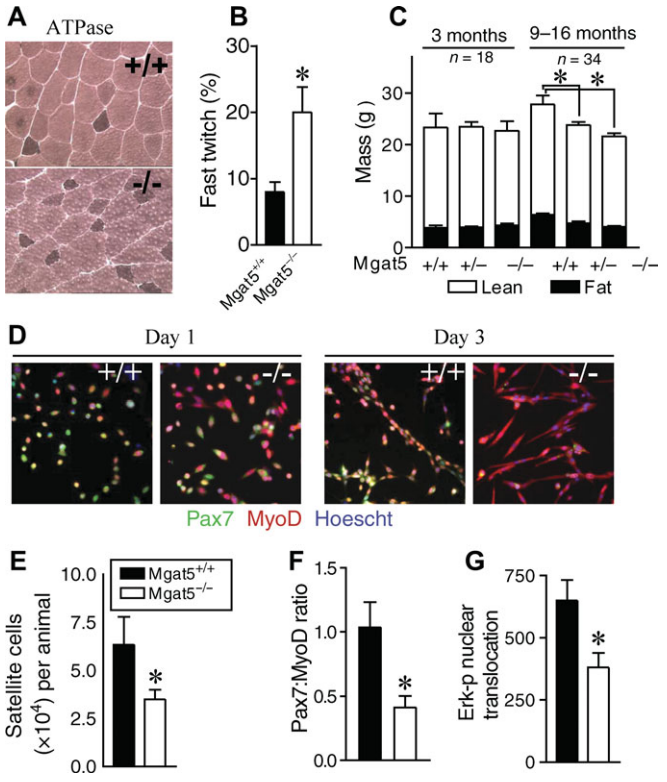

Fig. 6. Mgat5 promotes satellite cell survival and muscle growth with aging. (**A**) Sections of muscle quadriceps in 129/sv mice were stained for alkaline ATPase to reveal fast-twitch fibers. (**B**) Fraction of fast twitch fibers. (**C**) Lean and fat content at 3 and 9–16 months of age in 129/sv mice, determined by dual energy X-ray absorptiometry; $*P < 0.05$ for fat and lean compared with Mgat5$^{+/+}$ mice. (**D**) Pax7 and MyoD expression in early passage satellite cells at 24 and 72 h after passage. (**E**) Satellite cells recovered per animal at 1 week of age ($n = 5$). (**F**) Ratio of Pax7+ to MyoD+ satellite cells in Mgat5$^{+/+}$ and Mgat5$^{-/-}$ cultures at 24 h (mean ± SD, $n = 3$ cultures from independent mice, six replicate counts). (**G**) Erk-p nuclear translocation in serum-starved satellite cells (24 h) after stimulation with 10% serum for 10 min and determination by ArrayScan (mean ± SD for three cultures from independent mice; $*P < 0.05$).

Table I. Serology measurements of 1-year-old 129/sv mice

	Mgat5$^{+/+}$			Mgat5$^{+/-}$			Mgat5$^{-/-}$		
	Mean	SE	*n*	Mean	SE	*n*	Mean	SE	*n*
Sodium	135.20	1.47	10	135.56	1.06	16	137.00	1.54	8
Potassium	7.01	0.46	10	7.70	0.45	16	9.75	1.58	8
Chloride	106.00	0.55	5	108.33	0.92	12	106.00	1.98	6
Calcium	0.97	0.04	10	0.93	0.03	15	0.83	0.12	8
Creatine*	101.00	18.34	9	65.44	10.72	16	49.38	4.85	8
Glutamine	8.25	0.28	10	8.08	0.30	16	7.56	0.60	8
Lactate	5.13	0.34	10	5.14	0.26	16	4.64	0.36	8
Urea	7.79	0.43	10	9.30	0.70	15	9.08	0.62	8

$*P < 0.05$, pairwise *t* test.

were normal, whereas creatine was 41% lower in Mgat5$^{-/-}$ mice at around 1 year of age, which may reflect a reduction in muscle growth and renewal (Table I).

Satellite cells, positioned between basal lamina and the membrane of the myofibers, provide most of the regenerative potential of adult muscles. In response to injury, satellite cells are stimulated to proliferate and differentiate to form MyoD$^+$ myocytes and myotubes (Conboy et al. 2003). Fewer satellite cells were isolated from newborn Mgat5$^{-/-}$ mice compared with wild-type littermates, suggesting that either insufficient satellite stem cells are generated during embryogenesis or their renewal is deficient in postnatal life, or both (Figure 6D and E). The Pax7+ to MyoD+ ratio in Mgat5$^{-/-}$ and Mgat5$^{+/+}$ satellite cell cultures was 0.5:1 and 1:1, respectively, indicating a higher rate of differentiation in mutant cells (Figure 6F). At higher cell densities, Mgat5$^{+/+}$ satellite cells fuse at higher frequency to form MyoD$^+$ myotubules, but fusion was impaired in Mgat5$^{-/-}$ cultures even though the cells were largely MyoD$^+$ (Figure 6D). Mgat5$^{-/-}$ satellite cells were less sensitive to serum-dependent activation of Erk, consistent with a tendency to favor myodifferentiation over self-renewal (Figure 6G).

In Mgat5$^{-/-}$ bone marrow cultures, nuclear Erk-p was decreased and nuclear Smad2/3 increased upon stimulation with serum, consistent with reduced replicative potential (Figure 7A). TGF-β/Smad signaling is required for the later stages of osteoblast differentiation and mineralization, but elevated TGF-β signaling limits the early expansion of osteoprogenitor colonies (Binkert et al. 1999). Male and female Mgat5$^{-/-}$ mice display multiple features characteristic of early aging, including loss of bone mineral density (BMD) in vertebrae and femur and in whole-body measurements (Figure 7B). Bone mass content and BMD in whole-body scans were reduced by approximately 20% in Mgat5$^{-/-}$ mice over 1 year of age compared with their Mgat5$^{+/+}$ littermates (Supplementary Figures S1 and S2). Bone marrow stromal cells from 3-month-old mice were cultured under conditions that induce osteogenesis, and the Mgat5$^{-/-}$ cells displayed reduced calcium phosphate deposition compared with stromal cells from Mgat5$^{+/+}$ littermates, suggesting a deficiency in either osteoblast numbers or differentiation (Figure 7C). Longevity is reduced in Mgat5$^{-/-}$ mice (Figure 7D), and other age-related pathologies observed in

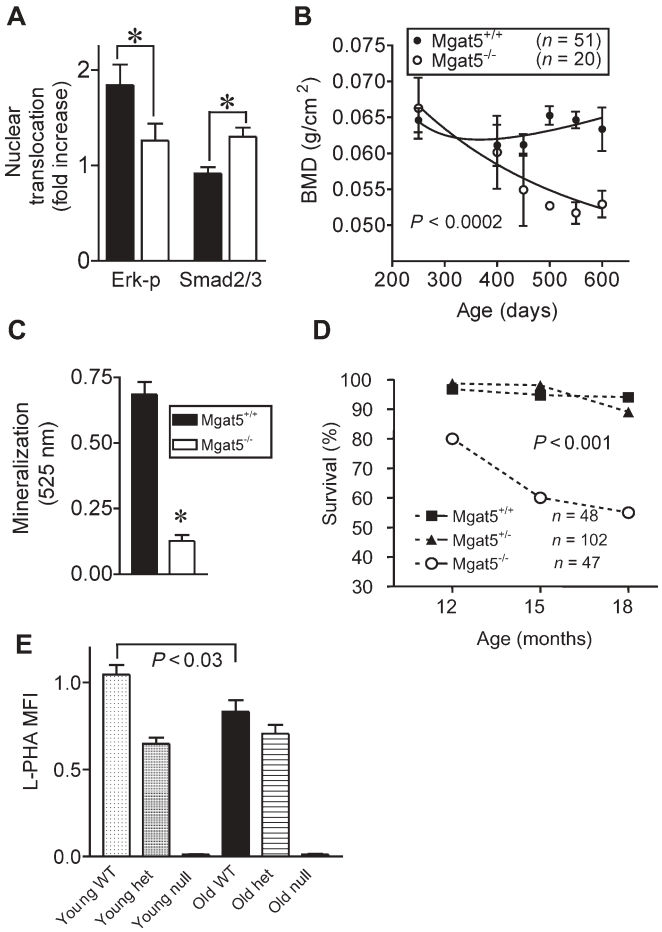

Fig. 7. Reduced osteogenesis in bone marrow cultures and osteoporosis in aging Mgat5$^{-/-}$ mice. (**A**) Fold increase in Erk-p and Smad2/3 nuclear translocation after 10 and 40 min of stimulation with serum, respectively. (**B**) Vertebra BMD in aging 129/sv Mgat5$^{+/+}$ and Mgat5$^{-/-}$ mice on the regular diet. (**C**) Osteogenesis in bone marrow stromal cell cultures from Mgat5$^{+/+}$ and Mgat5$^{-/-}$ mice at 3 months of age (mean ± SD, $n = 8$); *$P <$ 0.05. (**D**) Survival of 129/sv male mice with the indicated Mgat5 genotypes. (**E**) β1,6GlcNAc-branched *N*-glycans on CD8+ spleen cells from young (3 months) and old 129/sv (12–14 months) mice stained with FITC–L-PHA and analyzed by FACS.

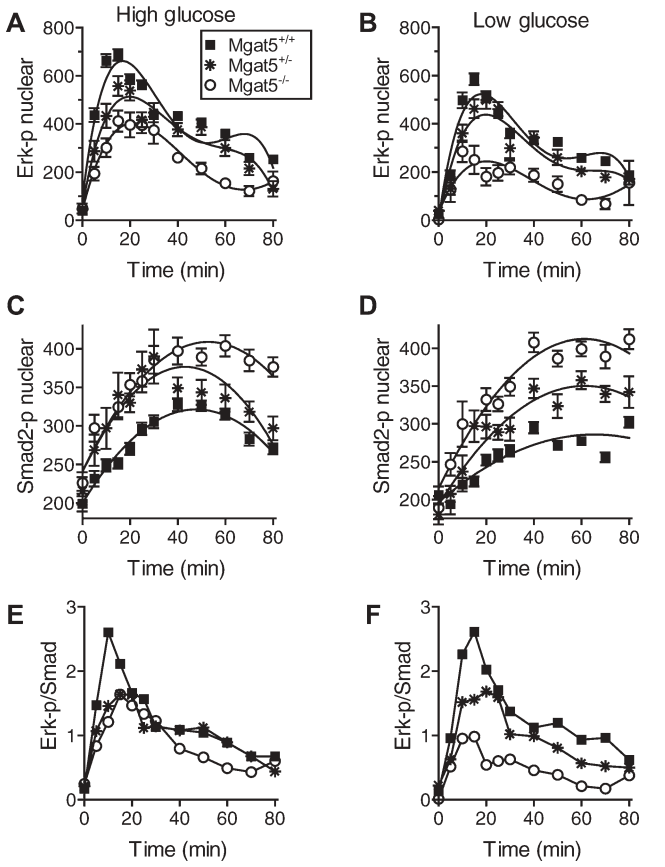

Fig. 8. Imbalanced RTK/Erk to TβR/Smad signaling in Mgat5$^{-/-}$ MEFs. [(**A**)–(**D**)] Nuclear localization of Erk-p and Smad2/3 in MEFs following stimulation with serum, measured by ArrayScan. MEFs were cultured in low- (0.5 mM) or high- (25 mM) glucose medium for 24 h, serum starved in the same medium for 24 h, and then stimulated with 10% serum for the time indicated on the *X*-axis. [(**E**) and (**F**)] Erk-p to Smad2/3 ratios generated from the primary data above each panel.

129/sv and C57Bl/6 Mgat5$^{-/-}$ mice include anal prolapse, excessive leanness, spinal compression or kyphosis, and excessive anxiety (Supplementary Table I). Expression of surface β1,6GlcNAc-branched *N*-glycans declines with aging in wild-type 129/sv mice but not in Mgat5$^{+/-}$ mice, as indicated by a lower L-PHA (*Phaseolus vulgaris* lectin L) reactivity of lymphocytes at 12 months of age compared with 3-month-old animals (Figure 7E).

Finally, a similar imbalance of Erk and Smad2/3 activation following serum stimulation of MEFs was observed in Mgat5$^{-/-}$ MEFs, with Mgat5$^{+/-}$ MEFs displaying an intermediate phenotype (Figure 8A–F). Low-glucose growth conditions further suppressed Erk activation in Mgat5$^{-/-}$ MEFs and prolonged Smad2/3 activation (Figure 8A–D). Our results suggest that β1,6GlcNAc-branched *N*-glycans promote self-renewal and pluripotency of stem cells by balancing signaling, including RTK/PI3K/Erk (growth and glycoytic metabolism) and TGF-β/Smad (arrest and differentiation) (Figure 9).

Discussion

Here, we report that Mgat5$^{-/-}$ mice are resistant to weight gain on an enriched diet, hypersensitive to fasting, mildly hypoglycemic, less fecund, and display reduced RQ while calorie intake and physical activity are normal. Tonic levels of activated Akt and Erk in Mgat5$^{-/-}$ MEFs under normal culture conditions as well as acute response to growth factors are reduced. Glucose uptake is impaired in Mgat5$^{-/-}$ MEFs under low-serum or low-glucose growth conditions, suggesting that Mgat5$^{-/-}$ MEFs are less resilient or adaptable to growth conditions. This suggests that Mgat5 *N*-glycan products enhance adoption to changes in nutrient conditions, which may include short-term shifts between anabolic and catabolic metabolism, as well as long-term adaptation.

Mgat5$^{-/-}$ MEFs display enhanced sensitivity to TGF-β and an apparent insufficiency in growth signaling, particularly in low-glucose conditions. TβRI/II complexes are rapidly recycled between the surface and endosomes, independent of their activation by ligand (Di Guglielmo et al. 2003). Hence, TGF-β signaling is particularly sensitive to membrane remodeling, which is stimulated by the growth-promoting RTKs. As such, surface levels of TβR can be increased to levels

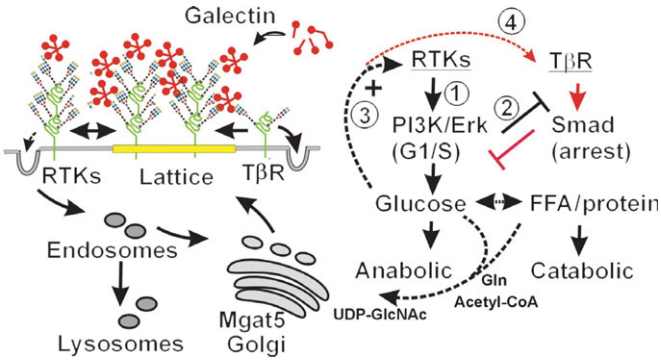

Fig. 9. Model of Mgat5/*N*-glycan processing-dependent regulation of growth and arrest cues. RTKs that promote growth have relatively high numbers of *N*-glycans with 11.4 ± 5.1 N-X-S/T consensus sequences ($n = 30$ receptors), estimated to be approximately 70% occupancy. TGF-β receptors types I and II have low multiplicity (1 and 2 N-X-S/T motifs, respectively) and therefore lower affinities for galectins (Lau et al. 2007). Receptor kinases with low multiplicity function in organogenesis and differentiation/arrest, and include Tie1, Musk, Ltk, ROR1/2, DDR1, the Eph receptors, and TGF-β/BMP receptors (27 receptors 2.48 ± 1.28 N-X-S/T sites/receptor). In Mgat5$^{-/-}$ cells, insufficient positive feedback to growth signaling (black) results in a predominance of arrest signaling (red). In wild-type cells, (1) stimulation of RTKs in quiescent cells; increased PI3K signaling promotes F-actin remodeling and (2) internalization of low-*n* receptors (e.g. TβR). (3) This enhances positive feedback to hexosamine/*N*-glycan processing, which leads ultimately to (4) increasing TβR association with galectins and autocrine arrest signaling.

that are functionally dominant for growth arrest by slowing endocytosis and/or increasing the hexosamine/Golgi/galectin lattice (Figure 9). In this regard, low-glucose conditions increased β1,6GlcNAc-branched *N*-glycans and UDP-GlcNAc levels (Figure 1F, data not shown). In low glucose, reduced protein synthesis and slower glycoprotein transit through the Golgi may spare UDP-GlcNAc and increase the fraction of β1,6GlcNAc-branched *N*-glycans. Although surface TβR and other arrest mediators may be functionally dominant under limiting conditions, the levels of growth-promoting high-*n* RTKs are also maintained by the lattice, and may serve to prime cells for a shift to more favorable growth conditions (Figure 9).

In vivo, Mgat5$^{-/-}$ mice displayed a significantly lower RQ during the rest period (light cycle) when serum glucose levels are generally lower. The Mgat5 deficiency did not impair β-cell function and insulin sensitivity, as suggested by normal glucose tolerance in Mgat5$^{-/-}$ mice. Skeletal muscle in adult Mgat5$^{-/-}$ mice displays characteristics of reduced glucose metabolism and, with aging, muscle and bone mass declined more rapidly compared with wild-type mice. The activation of Erk and Smad2/3 in Mgat5$^{-/-}$ MEFs and bone marrow stem cells by serum favored Smad2/3, suggesting that the Mgat5 deficiency increases the probability of growth arrest. In vivo, Mgat5$^{-/-}$ muscle displays pathology associated with reduced glycolytic metabolism consistent with a lower RQ, suggesting a shift toward increased metabolism of other carbon sources such as fatty acids and protein. Moreover, young Mgat5$^{-/-}$ mice are deficient in bone marrow osteogenesis and muscle satellite cells compared with age-matched wild-type littermates. In phosphatase and tensin homologue (Pten$^{+/-}$) mice in which PI3K/Akt growth signaling is increased, early overproliferation of stem cells is followed by their loss, which could be partially rescued by inhibiting downstream mTor kinase with rapamycin (Yilmaz et al. 2006). The deletion of the Rho GTPase Rac1 in epidermis, a pleiotropic regulator of growth signaling downstream of RTKs, stimulated stem cells to divide and then undergo terminal differentiation, thus a failure of maintenance and repair (Benitah et al. 2005). Taken with the present results, balancing growth and arrest signaling in stem cells and tissue renewal is dependent on conditional regulation of β1,6GlcNAc-branched *N*-glycans on glycoprotein receptors.

Moderate calorie restriction promotes longevity in *S. cerevisiae*, *Caenorhabditis elegans*, and mammals (Guarente and Picard 2005), and in yeast, minimizes storage and balances glycolytic and oxidative respiration to promote high-energy charge and low ROS (Lin et al. 2002). Mice with a single copy of the insulin receptor gene (IGF-1R) display normal energy metabolism and slightly longer lifespan (Holzenberger et al. 2003). Although the apparent reduction in glucose utilization in Mgat5$^{-/-}$ mice might be expected to extend longevity, the accompanying increase in oxidative respiration and reduced soft tissue mass with aging suggest a limiting defect in anabolic metabolism. Akt1-deficient mice also display a slow-growth phenotype but manifested at birth, whereas in Mgat5$^{-/-}$ mice, renewal and growth in adult mice is impaired (Cho et al. 2001). Pten phosphatase opposes intracellular PI3K/Akt signaling and is a potent tumor suppressor. The Mgat5-deficiency increases survival time by 8–40% in Pten$^{+/-}$ mice, suggesting that Mgat5$^{-/-}$ exerts a brake on hyperactivation of PI3K/Akt signaling and slows tumor development in the Pten$^{+/-}$ background (Cheung and Dennis 2007). Increased p53 activity also suppresses tumor development, and favors arrest signaling, oxidative metabolism, loss of stem cells, and early mortality (Tyner et al. 2002; van Heemst et al. 2005), features common with the Mgat5$^{-/-}$ phenotype. *N*-glycan processing, PI3K/Pten, and p53 appear to be highly integrated with signaling networks and basic metabolism.

The allosteric feedback regulation of enzymes by metabolites occurs on a timescale of seconds, whereas changes in *N*-glycan biosynthesis and turnover of surface glycoproteins are slower. Mgat5 and *N*-glycan processing may adapt cellular sensitivity to cytokines by functioning both upstream and downstream of metabolism, thereby impacting body weight, fecundity, stem cell renewal, and aging. The efficient utilization and storage of nutrients when food is abundant increases the probability of survival in the capricious environments that characterize most of natural history. However, the rise in obesity and type-2 diabetes with the Western lifestyle indicates a strong interaction between genes and the nutrient environment (Diamond 2003; O'Rahilly et al. 2005). Further analysis of metabolite flux to sugar-nucleotide and *N*-glycan branching may suggest new avenues to enhance productive lifespan through stem cell maintenance and suppression of obesity.

Materials and methods

Mice and cell lines

The Mgat5 mutation was maintained on C57BL/6 and 129/sv backgrounds, backcrossed 10 generations (Granovsky et al.

2000). The C57BL/6 background is hypersensitive to obesity and insulin resistance on a high-fat diet, and was adopted for the diet experiments in Figures 2 and 3. The 129/sv strain was used for the generation of MEFs and for all other experiments in this report. The Mgat5 mutation had similar effects on reducing fecundity and early mortality on both strain backgrounds. Mice were fed the regular diet unless stated otherwise, which was gram percent of 38.6% starch, 22.5% protein, 9% fat, with a metabolizable energy of 3.11 kcal/g (LabDiet® 5012, Purina Mills, St. Louis, MO). The enriched diet comprised 38% starch, 20.5% protein, 18.5% fat for a metabolizable energy of 3.82 kcal/g (PicoLab® mouse diet 20, Purina Mills) with an additional 6% dry supplement of sucrose. Daily food intake per animal was determined every 24 h over 10 days and expressed per body mass corrected by power function (g baseline weight)$^{0.568}$, as described previously (Conti et al. 2006). MEFs were isolated from E14.5 embryos from Mgat5$^{+/-}$ × Mgat5$^{+/-}$ matings using standard protocols and cultured in Dulbecco's modified Eagle's medium (DMEM) containing 10% FCS (serum) (Invitrogen, Carlsbad, CA). After two passages, the MEFs were cryopreserved in 10% dimethyl sulfoixde (DMSO)–20% FCS in DMEM and used in experiments after no more than two further passages or 2 weeks in culture.

Nuclear translocation of Erk-p and Smad2/3

Cells plated in 96-well plates at 1000 cells/well were serum-starved for 24 h and then stimulated with TGF-β1, EGF (R&D Systems, Minneapolis, MN), or serum. Cells were fixed after 40 min of TGF-β stimulation to measure Smad2/3 nuclear translocation, or after 5 min of EGF stimulation to measure Erk-p nuclear translocation. Cells were fixed for 10 min with 3.7% formaldehyde at room temperature, washed with phosphate-buffered saline (PBS) plus 1% serum, and permeabilized using 100% MeOH for 2 min. The cells were washed 3 times and blocked in PBS plus 10% serum overnight at 4 °C. Mouse anti-Smad2/3 (Transduction Laboratories S66220, BD Biosciences, San Jose, CA) or mouse phospho-Erk1/2 (Thr202/Tyr204) (Sigma M-8159) or antiphospho Smad2 (Ser465/467) (Cell Signaling 3101S, Technology, Danvers, Sigma-Aldrich, St. Louis, MO) was added at 1/1000 in PBS plus 10% serum for 2 h at 20 °C. The cells were washed 3 times with PBS plus 1% serum. AlexaFluor 488-labeled antimouse Ig secondary antibody (Molecular Probes) was added at 1/1000 with Hoechst 33342 (1/2000) (Molecular Probes, Invitrogen) for 1 h at 20 °C. After washing 3 times, the plates were scanned using the ArrayScan II fluorescence microscope (Cellomics, Pittsburgh). The nuclear and cytoplasmic staining intensities were determined individually for 200 cells/well and cytoplasmic staining intensity subtracted from nuclear staining intensity for each cell. The mean differential signal ± SE ($n = 200$) was generally <4% at each assay point.

Spleen cells from 129/sv were stained with 10 ng/mL of fluorescein isothiocyanate (FITC) L-PHA (E-Y Labs, San Mateo, CA) and tetramethylrhodamine isothiocyanate (TRITC)-anti-CD8 (eBioscience, San Diego, CA) at room temperature for 1 h and then fixed without permeabilization. Cells were analyzed by fluorescence activated cell sorting (FACS), and L-PHA mean fluorescence intensity in CD8+ cells was quantified.

Glucose transport and ROS measurements

Cells were seeded in triplicate at 2.5×10^5 cells/well in six-well plates. Following incubation at 37 °C, the cells were washed twice with assay buffer (Krebs–Ringer solution: 116 mM NaCl, 5.4 mM KCl, 0.8 mM $MgSO_4$, 1.0 mM $CaCl_2$, 25 mM Tris–HCl, 0.2% bovine serum albumin (BSA), 1.0 mM NaH_2PO_4, and 2.0 mM Na_2PO_4, pH 7.45). Cells were then incubated with assay buffer (1 mL/well) at 37 °C for 30 min, with the addition of 1 mL of [^{3}H]2-deoxy-D-glucose (2 μCi/mL) (NEN) in assay buffer for a further 20 min. The cells were washed 4 times with ice-cold assay buffer, and 0.5 mL of ice-cold 5% trichloroacetic acid (TCA) was added to each well. After 30 min on ice, 0.4 mL of TCA supernatant was removed and [^{3}H]2-deoxy-D-glucose was quantified by scintillation counting.

To measure ROS, cells were seeded in triplicate at a density of 1000 cells/well in 96-well plates (Corning 96 Flat Opaque, Corning, NY) and cultured for 24 h. Cells were washed with PBS, followed by the addition of 100 μl of 1 μM H_2DCFDA (Molecular Probes, Invitrogen) in PBS. The plates were incubated at 37 °C for 30 min, and oxidized probe at the bottom of each well was determined by excitation at 485–20 nm and emission was measured at 530–25 nm using an Analyst HT plate reader (Molecular Devices) and the Criterion Host software (LJL Biosystems, Molecular Devices Corporation, Sunnyvale, CA). Background fluorescence in the absence of probe was subtracted, and a standard curve for oxidation was generated using hydrogen peroxide. Results are plotted as the mean ± SD of triplicate determinations, and experiments were repeated 3 times.

Respiratory quotient

Oxygen consumption and carbon dioxide production rates were recorded every 15 min for 24 h with the use of a mouse indirect calorimeter (Oxymax; Columbus Instruments, Columbus, OH). Water and food (regular diet) were available ad libitum in the chambers. Measurements were taken in an airtight Oxymax chamber with an airflow rate of 0.5 L/min. RQ was calculated as the molar ratio of $V\mathrm{co}_2$ to $V\mathrm{o}_2$ for 10 mice per genotype, averaging the 15 min measurements for the light and dark cycle CO_2 and O_2. Locomotion and total movement were measured continuously during the 24 h. Locomotion is a measure of lateral movement, whereas total movement includes body movements such as grooming as well as lateral movement.

Muscle and satellite cells

Satellite cells were extracted from the muscle of the limbs by incubating with collagenase–dispase solution (Hoffmann–La Roche, Basal, Switzerland) for 30 min with agitation. Fibroblasts were removed by adherence to tissue culture plates in Ham's F-10 (Invitrogen) incubated for 60 min at 37 °C. The non-adhering satellite cells were transferred to collagen-coated dishes and cultured in Ham's F-10 medium, 20% serum, penicillin/streptomycin, Fungizone (Invitrogen), and 20 nM bFGF (Sigma).

For immunohistochemistry, satellite cells were plated onto collagen-coated glass coverslips and cultured for 1–4 days in the earlier-mentioned medium. Slides were fixed with 3.7% formaldehyde in PBS and permeabilized with cold

100% methanol for 2 min, and blocked in PBS, 10% serum overnight at 4 °C. Cells were stained with a 1 : 50 dilution of mouse anti-Pax7 (Developmental Studies Hybridoma Bank, Iowa City, IA) and 1 : 50 rabbit anti-MyoD (Santa Cruz Biotechnology, Santa Cruz, CA) diluted in PBS, 10% serum for 2 h at room temperature. Slides were washed with PBS, 10% serum and stained with 1 : 100 AlexaFluor 488 goat anti-mouse Ig, and Cy5-labeled goat antirabbit Ig (Jackson Labs, The Jackson Laboratory, Bar Harbor, ME) and 1: 500 Hoechst for 30 min at room temperature. Slides were washed, mounted, and imaged. Cryosections of quadriceps muscle (8 μm) were mounted, postfixed with 4% paraformaldehyde, and stained for alkaline ATPase, pH 9.4, which stained fast-twitch myofibers darkly, whereas slow-twitch myofibers stained lightly.

Bone phenotype and osteogenesis in bone marrow cultures

Dual-energy X-ray absorptiometry (Pixi mus, Fitchburg, WI; GE Healthcare Bio-Sciences, Piscataway, NJ) was used to measure bone mineral content, bone area, and BMD on whole animals. Femurs were removed under aseptic conditions from mice, cleaned of adherent soft tissues, and washed extensively in antibiotics. The distal ends were removed and the marrow contents were flushed out with 10 mL of culture medium. Cells were dispersed by repeated passage through a 20-gauge needle and incubated in alpha-MEM supplemented with 15% serum, ascorbic acid (50 μg/mL), antibiotics [penicillin G 100 μg/mL, gentamicin 50 μg/mL, Fungizone (Invitrogen) 0.3 μg/mL], 10 mM β-glycerophosphate, and vitamin C. Culture media was supplemented further with dexamethasone (10^{-8} M). Following 6 days of culture, the cells were replated at a density of 1×10^2 cells/mm^2 in 96-well plates and grown for another 12–14 days, with changes of the same medium at 48 h intervals. At the end of culture, the cells were fixed with 10% buffered formalin and stained for calcium with Alizarin red-S to identify mineralized bone nodules. To quantify mineralized tissue formation in the cultures, the absorbance at 525 nm was measured using a 96-well plate reader. Duplicate wells were stained for lipid content. Cells were fixed with 70% ethanol and stained with Sudan IV in acetone:ethanol for 20 min and washed with 70% ethanol for photographic documentation.

Supplementary data

Supplementary data are available at Glycobiology online http://glycob.oxfordjournals.org/).

Acknowledgments

This research was supported by grants to J.W.D. from the Canadian Institute for Health Research. The authors thank Susan Wang, Dr Luisa Moreno, Lois Kelsey, and Laili Soleimani for technical assistance.

Conflict of interest statement

None declared.

Abbreviations

bFGF, fibroblast growth factor; BMD, bone mineral density; BMP, bone morphogenic protein; DMEM, Dulbecco's modified Eagle's medium; EGFR, epidermal growth factor (EGF) receptor; Erk, extracellular response kinase; FCS, fetal calf serum; FITC, fluorescein isothiocyanate; GlcNAc-T, *N*-acetylglucosaminyltransferase; IGF, insulin-like growth factor; L-PHA, *Phaseolus vulgaris* lectin L; MEF, mouse embryonic fibroblast; Mgat5, β1,6-*N*-acetylglucosaminyltransferase V gene; PBS, phosphate-buffered saline; PDGF, platelet-derived growth factor; PI3K, phosphoinositide 3-kinase; Pten, phosphatase and tensin homolog; ROS, reactive oxygen species; RQ, respiratory quotient; RTK, receptor tyrosine kinase; SFM, serum-free medium; TβR, transforming growth factor-β receptor; UDP-GlcNAc, UDP-*N*-acetylglucosamine

References

Benitah SA, Frye M, Glogauer M, Watt FM. 2005. Stem cell depletion through epidermal deletion of Rac1. Science. 309:933–935.

Binkert C, Demetriou M, Sukhu B, Szweras M, Tenenbaum HC, Dennis JW. 1999. Regulation of osteogenesis by fetuin. J Biol Chem. 274: 28514–28520.

Brewer CF, Miceli MC, Baum LG. 2002. Clusters, bundles, arrays and lattices: novel mechanisms for lectin-saccharide-mediated cellular interactions. Curr Opin Struct Biol. 12:616–623.

Brown JR, Ye H, Bronson RT, Dikkes P, Greenberg ME. 1996. A defect in nurturing in mice lacking the immediate early gene fosB. Cell. 86: 297–309.

Buckhaults P, Chen L, Fregien N, Pierce M. 1997. Transcriptional regulation of *N*-acetylglucosaminyltransferase V by the src oncogene. J Biol Chem. 272:19575–19581.

Campisi J. 2005. Senescent cells, tumor suppression, and organismal aging: good citizens, bad neighbors. Cell. 120:513–522.

Cheung P, Dennis JW. 2007. Mgat5 and Pten interact to regulate cell growth and polarity. Glycobiology. 17:767–773.

Cho H, Thorvaldsen JL, Chu Q, Feng F, Birnbaum MJ. 2001. Akt1/PKBalpha is required for normal growth but dispensable for maintenance of glucose homeostasis in mice. J Biol Chem. 276:38349–38352.

Conboy IM, Conboy MJ, Smythe GM, Rando TA. 2003. Notch-mediated restoration of regenerative potential to aged muscle. Science. 302:1575–1577.

Conboy IM, Conboy MJ, Wagers AJ, Girma ER, Weissman IL, Rando TA. 2005. Rejuvenation of aged progenitor cells by exposure to a young systemic environment. Nature. 433:760–764.

Conti B, Sanchez-Alavez M, Winsky-Sommerer R, Morale MC, Lucero J, Brownell S, Fabre V, Huitron-Resendiz S, Henriksen S, Zorrilla EP, et al. 2006. Transgenic mice with a reduced core body temperature have an increased life span. Science. 314:825–828.

Demetriou M, Granovsky M, Quaggin S, Dennis JW. 2001. Negative regulation of T-cell activation and autoimmunity by Mgat5 N-glycosylation. Nature. 409:733–739.

Diamond J. 2003. The double puzzle of diabetes. Nature. 423:599–602.

Di Guglielmo GM, Le Roy C, Goodfellow AF, Wrana JL. 2003. Distinct endocytic pathways regulate TGF-beta receptor signalling and turnover. Nat Cell Biol. 5:410–421.

Di Paolo G, De Camilli P. 2006. Phosphoinositides in cell regulation and membrane dynamics. Nature. 443:651–657.

Dobrzyn P, Dobrzyn A, Miyazaki M, Cohen P, Asilmaz E, Hardie DG, Friedman JM, Ntambi JM. 2004. Stearoyl-CoA desaturase 1 deficiency increases fatty acid oxidation by activating AMP-activated protein kinase in liver. Proc Natl Acad Sci USA. 101:6409–6414.

Fernandes B, Sagman U, Auger M, Demetriou M, Dennis JW. 1991. Beta1-6 branched oligosaccharides as a marker of tumor progression in human breast and colon neoplasia. Cancer Res. 51:718–723.

Granovsky M, Fata J, Pawling J, Muller WJ, Khokha R, Dennis JW. 2000. Suppression of tumor growth and metastasis in Mgat5-deficient mice. Nat Med. 6:306–312.

Grigorian A, Lee S-U, Tian W, Chen I-J, Guoyan G, Mendelsohn R, Dennis JW, Demetriou M. May 8, 2007. Control of T cell mediated autoimmunity by metabolite flux to *N*-glycan. J Biol Chem. doi:10.1074/jbc.M701890200.

Guarente L, Picard F. 2005. Calorie restriction—the SIR2 connection. Cell. 120:473–482.

Hager R, Johnstone RA. 2003. The genetic basis of family conflict resolution in mice. Nature. 421:533–535.

Hirabayashi J, Hashidate T, Arata Y, Nishi N, Nakamura T, Hirashima M, Urashima T, Oka T, Futai M, Muller WE, et al. 2002. Oligosaccharide specificity of galectins: a search by frontal affinity chromatography. Biochim Biophys Acta. 1572:232–254.

Holzenberger M, Dupont J, Ducos B, Leneuve P, Geloen A, Even PC, Cervera P, Le Bouc Y. 2003. IGF-1 receptor regulates lifespan and resistance to oxidative stress in mice. Nature. 421:182–187.

Jin SH, Blendy JA, Thomas SA. 2005. Cyclic AMP response element-binding protein is required for normal maternal nurturing behavior. Neuroscience. 133:647–655.

Kang R, Saito H, Ihara Y, Miyoshi E, Koyama N, Sheng Y, Taniguchi N. 1996. Transcriptional regulation of the *N*-acetylglucosaminyltranserase V gene in human bile duct carcinoma cells (HuCC-T1) is mediated by Ets-1. J Biol Chem. 271:26706–26712.

Kilner RM, Madden JR, Hauber ME. 2004. Brood parasitic cowbird nestlings use host young to procure resources. Science. 305:877–879.

Lau K, Partridge EA, Silvescu CI, Grigorian A, Pawling J, Reinhold VN, Demetriou M, Dennis JW. 2007. Complex *N*-glycan number and degree of branching cooperate to regulate cell proliferation and differentiation. Cell. 129:123–134.

Lin S-J, Kaeberlein M, Andalis AA, Sturtz LA, Defossez P-A, Culotta VC, Fink GR, Guarente L. 2002. Calorie restriction extends *Saccharomyces cerevisiae* lifespan by increasing respiration. Nature. 418:344–348.

Matoba S, Kang JG, Patino WD, Wragg A, Boehm M, Gavrilova O, Hurley PJ, Bunz F, Hwang PM. 2006. p53 regulates mitochondrial respiration. Science. 312:1650–1653.

O'Rahilly S, Barroso I, Wareham NJ. 2005. Genetic factors in type 2 diabetes: the end of the beginning? Science. 307:370–373.

Ozcan S, Dover J, Johnston M. 1998. Glucose sensing and signaling by two glucose receptors in the yeast *Saccharomyces cerevisiae*. EMBO J. 17:2566–2573.

Parker GA, Royle NJ, Hartley IR. 2002. Intrafamilial conflict and parental investment: a synthesis. Philos Trans R Soc Lond B Biol Sci. 357:295–307.

Partridge EA, Le Roy C, Di Guglielmo GM, Pawling J, Cheung P, Granovsky M, Nabi IR, Wrana JL, Dennis JW. 2004. Regulation of cytokine receptors by Golgi *N*-glycan processing and endocytosis. Science. 306:120–124.

Piccirillo SG, Reynolds BA, Zanetti N, Lamorte G, Binda E, Broggi G, Brem H, Olivi A, Dimeco F, Vescovi AL, et al. 2006. Bone morphogenetic proteins inhibit the tumorigenic potential of human brain tumour-initiating cells. Nature. 444:761–765.

Rolland F, De Winde JH, Lemaire K, Boles E, Thevelein JM, Winderickx J. 2000. Glucose-induced cAMP signalling in yeast requires both a G-protein coupled receptor system for extracellular glucose detection and a separable hexose kinase-dependent sensing process. Mol Microbiol. 38:348–358.

Ryder JW, Bassel-Duby R, Olson EN, Zierath JR. 2003. Skeletal muscle reprogramming by activation of calcineurin improves insulin action on metabolic pathways. J Biol Chem. 278:44298–44304.

Sasai K, Ikeda Y, Fujii T, Tsuda T, Taniguchi N. 2002. UDP-GlcNAc concentration is an important factor in the biosynthesis of beta1,6-branched oligosaccharides: regulation based on the kinetic properties of *N*-acetylglucosaminyltransferase V. Glycobiology. 12:119–127.

Seelentag WK, Li WP, Schmitz SF, Metzger U, Aeberhard P, Heitz PU, Roth J. 1998. Prognostic value of beta1,6-branched oligosaccharides in human colorectal carcinoma. Cancer Res. 58:5559–5564.

Seoane J, Le HV, Shen L, Anderson SA, Massague J. 2004. Integration of Smad and forkhead pathways in the control of neuroepithelial and glioblastoma cell proliferation. Cell. 117:211–223.

Siegel PM, Massague J. 2003. Cytostatic and apoptotic actions of TGF-beta in homeostasis and cancer. Nat Rev Cancer. 3:807–821.

Sobko A. 2006. Systems biology of AGC kinases in fungi. Sci STKE. 352: re9.

Tyner SD, Venkatachalam S, Choi J, Jones S, Ghebranious N, Igelmann H, Lu X, Soron G, Cooper B, Brayton C, et al. 2002. p53 mutant mice that display early ageing-associated phenotypes. Nature. 415:45–53.

van Heemst D, Mooijaart SP, Beekman M, Schreuder J, de Craen AJ, Brandt BW, Slagboom PE, Westendorp RG. 2005. Variation in the human TP53 gene affects old age survival and cancer mortality. Exp Gerontol. 40:11–15.

Wakefield LM, Roberts AB. 2002. TGF-beta signaling: positive and negative effects on tumorigenesis. Curr Opin Genet Dev. 12:22–29.

Xu RH, Peck RM, Li DS, Feng X, Ludwig T, Thomson JA. 2005. Basic FGF and suppression of BMP signaling sustain undifferentiated proliferation of human ES cells. Nat Methods. 2:185–190.

Yeo EJ, Park SC. 2002. Age-dependent agonist-specific dysregulation of membrane-mediated signal transduction: emergence of the gate theory of aging. Mech Ageing Dev. 123:1563–1578.

Yilmaz OH, Valdez R, Theisen BK, Guo W, Ferguson DO, Wu H, Morrison SJ. 2006. Pten dependence distinguishes haematopoietic stem cells from leukaemia-initiating cells. Nature. 441:475–482.